

Morphology and methanol permeability of sulfosuccinic acid cross-linked polyvinyl alcohol and polyvinyl alcohol/Nafion nanofibrous membranes

Mert Işlay^{1,2}  | Ahmet Çay³  | Çiğdem Akduman⁴  |
Emriye Perrin Akçakoca Kumbasar³  | Hasan Ertaş⁵ 

¹Graduate School of Natural and Applied Sciences, Department of Textile Engineering, Ege University, Bornova, İzmir, Turkey

²Faculty of Engineering, Department of Textile Engineering, Dokuz Eylül University, Buca, İzmir, Turkey

³Faculty of Engineering, Department of Textile Engineering, Ege University, Bornova, İzmir, Turkey

⁴Department of Textile Technology, Denizli Vocational School of Technical Sciences, Pamukkale University, Denizli, Turkey

⁵Faculty of Science, Department of Chemistry, Ege University, Bornova, İzmir, Turkey

Correspondence

Ahmet Çay, Department of Textile Engineering, Faculty of Engineering, Ege University, Bornova, İzmir, Turkey.
Email: ahmet.cay@ege.edu.tr

Funding information

Ege University Research Foundation, Grant/Award Number: FYL-2019-21411

Abstract

Cross-linking of polyvinyl alcohol (PVA) and polyvinyl alcohol/Nafion (PVA/Nafion) electrospun nanofibers with sulfosuccinic acid (SSA) was investigated to assess their characterization and the effects of cross-linking on the methanol permeability performance of the nanofibrous membranes. SSA was directly incorporated into the electrospinning polymer solution. The morphology, chemical functional groups, thermal stability, water stability and water swelling of the resulting nanofibers were examined. The effects of SSA concentration on ion exchange capacity (IEC) and methanol permeability of the nanofibrous membranes were discussed. Bead-free and smooth nanofibers were produced for all SSA concentrations with a mean nanofiber diameter of 240–270 nm. It was shown that 15% SSA concentration was suitable for preserving the morphology of PVA nanofibers against water, while the morphology of PVA/Nafion nanofibers was preserved even without cross-linking. The increase in SSA concentration led to increase in swelling in water. SSA cross-linking was also shown to increase the thermal stability of the produced nanofibers. IEC increased by the increase in SSA concentration, while increase in SSA concentration led to a decrease in methanol permeability.

KEYWORDS

electrospinning, methanol permeability, Nafion, nanofiber, polyvinyl alcohol, sulfosuccinic acid

1 | INTRODUCTION

Electrospun nanofibrous membranes represent a cutting-edge advancement in the field of membrane technology, offering several potential applications in various industries, including energy storage,¹ fuel cells,^{2,3} sensors,⁴ filtration,^{5–7} water purification⁸ and biomedical devices.^{9,10} These membranes, composed of polymer nanofibers, exhibit unique characteristics such as high surface area-to-volume ratio, tunable pore size distribution, and enhanced

mechanical strength, making them highly desirable for a range of technological applications. Nanofiber technology offers several advantages, including the ease of production through the electrospinning method, versatility in producing nanofibers from a diverse range of polymers, and the convenience of functionalization.^{11–13} Regarding these areas, recent research draws attention to the potential use of electrospun nanofibrous membranes or their composites as polymer electrolyte membranes in fuel cells.^{3,14,15}

Today, the most commonly used membrane in polymer electrolyte membrane fuel cells (PEMFCs) and direct methanol fuel cells (DMFCs) is Nafion based film membranes.¹⁶ Nafion is a brand name for a type of perfluorinated sulfonic acid polymer. It is a highly fluorinated polymer made from tetrafluoroethylene and perfluoro-3,6-dioxo-4-methyl-7-octenesulfonic acid.¹⁷ Like most fluoropolymers, Nafion is known for its remarkable properties, including high thermal stability, excellent chemical resistance, and most importantly, its high proton conductivity, which makes it suitable for fuel cells, electrolyzers, batteries, and other electrochemical devices. However, the drawbacks such as high price, poor water management and high methanol permeability¹⁸ of Nafion films have led the researchers to investigate alternative membrane materials and structures. It has been demonstrated that the use of a nanofibrous form contribute to ionic alignment by supporting the orientation of the polymer during electrospinning, which helps the formation of long proton conduction channels within the membrane.^{19–21} Dong et al.²² showed that when Nafion was converted into a nanofiber structure, the proton conductivity increased compared to the film membrane. In addition, a decrease in methanol permeability is possible by acting as a barrier against the passage of fuel (methanol) owing to the entanglement of the nanofibrous structure.²¹

It is not possible to electrospun Nafion alone into nanofiber due to the insufficient chain entanglements arising from the aggregate formation by electrostatic forces¹⁵; therefore, a carrier polymer is needed during electrospinning of Nafion nanofibers. It should be noted that the carrier polymer should also have proton conduction property; therefore, it is required to use a polymer that contains a sulfonic acid group or that can be subsequently sulfonated. Considering this issue, polyvinyl alcohol (PVA) is a suitable carrier polymer for Nafion nanofibers because of its ease in preparing aqueous electrospinning solutions and its ability to be sulfonated. PVA was also reported to be effective for reducing the fuel crossover and permeability because of the long-bond chain polymeric matrix.²³ The affinity of PVA for water is higher than alcohols, which supports the reduction in methanol diffusion through the membranes.²⁴ Therefore, there have been a variety of studies on the use of PVA and PVA/Nafion based nanofibers as polymer electrolyte membranes.^{25–29} Despite all its advantages, an additional chemical or physical stabilization process is required since PVA is a water-soluble polymer. In addition, in order to be used in fuel cells, it must undergo a further sulfonating process. In this study, the use of sulfosuccinic acid (SSA) for chemical stabilization was investigated. Since SSA contains a sulfonic acid groups along with two

carboxylic acid groups, it is possible to obtain stabilization and sulfonation simultaneously. There are numerous studies on the use of SSA for PVA stabilization for film membranes obtained by solution casting method^{30–34}; however, unlike film membranes, electrospun membranes have a nanofibrous morphology and the preservation of the nanofibrous structure after stabilization against water is of great importance. Therefore, information obtained from film membrane research would not be categorically valid for nanofibrous ones. When nanofiber studies were examined, it was observed that the application of SSA for PVA electrospun nanofibers was only appeared in the study of Gil-Castell et al.³⁵ In their study, PVA nanofibers including graphene oxide were cross-linked and sulfonated by SSA and their morphology and proton conductivity were analyzed. However, the effects of SSA concentration and methanol permeability of the resultant nanofibrous membranes were not investigated. Besides, no study was encountered on the SSA cross-linked PVA/Nafion nanofibers. Therefore, in this study, PVA and PVA/Nafion nanofibers were cross-linked with SSA and the effects of SSA concentration on the morphology, preservation of the nanofibrous structure, water swelling and resulting methanol permeability were investigated for the first time to the best of the authors' knowledge.

2 | EXPERIMENTAL

2.1 | Materials

PVA (Mowiol® 20-98, 125,000 g/mol), Nafion® 117 solution (~5% in a mixture of lower aliphatic alcohols and water), sulfosuccinic acid (70 wt% in H₂O) and sodium hypophosphite monohydrate (NaH₂PO₂·H₂O) were purchased from Sigma Aldrich.

2.2 | Electrospinning

Stock solution of 10% PVA (w/v) was prepared by dissolving of PVA polymer in distilled water by stirring at 80°C for at least 3 h. After the solution was cooled down to room temperature, 0.05 mL/g_{polymer} Tween 80® was added to reduce the surface tension. SSA with different concentrations (5%, 10% and 15% by polymer weight) was directly added into the PVA electrospinning solution with sodium hypophosphite monohydrate as catalyst in ratio of 2:1. SSA concentrations higher than 15% was not selected because of the possibility of unstable jet stream formation during electrospinning due to high conductivity³⁶ and inhibition of the formation of continuous jets

due to the protonation of PVA under highly acidic conditions.³⁷

In order to prepare PVA/Nafion electrospinning solutions, different amounts of SSA incorporated PVA solutions were mixed with 5% Nafion solution with a ratio of 1:1 by volume.

Nanofibers were produced using an electrospinning device (Nanospinner, NS Plus, Inovenso), which includes a high voltage power supply connected to the needle tips, two feeding units and a collector unit that can function as a rotating cylinder or flat metal. For nanofiber production, 2.5 cm long and 22 gauge thick needles with blunt ends were employed. Electrospinning was carried out at a voltage of 18 kV, a polymer feeding rate of 0.7 mL/h and a tip-to collector distance of 15 cm. The produced nanofibers were collected on a stationary rectangular flat metal collector covered with aluminum foil. Electrospinning process was continued till the membranes reached 0.12 mm thickness. Afterwards, nanofibrous membranes were separated from aluminum foil and subjected to heat treatment in an oven at 180°C for 15 min to complete the crosslinking reaction of PVA and SSA. In order to fully understand the effect of SSA, neat PVA and PVA/Nafion nanofibers without SSA were also produced with the same electrospinning and heat treatment procedure.

2.3 | Tests and characterization

The viscosity of the electrospinning solutions was measured using a Brookfield DV III rheometer with a SC4-21 spindle at 30 rpm. The conductivity and pH of the solutions were tested by a J.P. Selecta (CD-2004) conductivity meter and a J.P. Selecta pH meter, respectively.

The morphology of the produced nanofibrous membranes was investigated by scanning electron microscope (SEM, Thermo Scientific Apreo S). Each sample was coated with a thin film of gold using a Leica EM ACE600 ion sputtering device before SEM analysis. The diameters of the produced nanofibers were measured by Image J Imaging and Measurement Software using SEM images. Fifty measurements were carried out on the different parts of each sample.

Fourier transfer infrared spectroscopy (FTIR) analysis was carried out to prove the esterification of PVA and SSA and incorporation of sulfonic acid groups into the structure using a PerkinElmer, Spectrum 100 FTIR spectrometer.

The thermal behavior of PVA and PVA/Nafion nanofibrous membranes crosslinked with SSA was investigated by thermogravimetric analysis using SDT

Q600 thermogravimetric analysis (TGA) device (TA Instruments) by heating samples from room temperature to 600°C under continuous nitrogen flow with a heating rate of 10°C/min.

In order to examine the durability of the membranes in water, the membranes were tested against water at room temperature and boiled water. The membranes were immersed in water for 1 h, separately. Then, the membranes were dried in an oven at 60°C for 24 h. Weight loss of the samples were calculated according to Equation (2), where M_0 is the initial dry weight of the samples and M_1 the dry weight obtained after the test. The weight loss in methanol solution test was carried out by the same procedure, but with a 5 M methanol solution at 80°C, and by using Equation (2).

$$\text{Weight loss} = \frac{M_0 - M_1}{M_0} \times 100. \quad (1)$$

To determine the swelling of the membranes in water, they were immersed in distilled water at room temperature for 24 h. After the treatment, their surface water was removed with a piece of filter paper and the weight of the swollen samples was measured. After that, they were dried in an oven at 60°C for 24 h. The swelling (%) was calculated using Equation (1), where M_1 is the dry weight after drying, M_s is the weight of swollen samples.

$$\text{Swelling (\%)} = \frac{M_s - M_1}{M_1} \times 100. \quad (2)$$

The ion exchange capacity (IEC) and the methanol permeability tests were applied to the membranes. For this purpose, the samples were first immersed into 1 M H₂SO₄ solution and boiled for 1 h to activate the membranes, followed by rinsing with boiling water for 15 min and drying at room temperature. The IEC tests were carried out according to titration method.^{38,39} The nanofibrous membranes were immersed into 2 M NaCl solution for 48 h. The solution, then, was titrated with 0.01 M NaOH solution using phenolphthalein as an indicator. The IEC of the membranes was calculated according to Equation (3), where V_{NaOH} is the volume of NaOH consumed during titration, M_{NaOH} is the molarity and W_0 is the initial dry membrane weight.

$$\text{IEC} = V_{\text{NaOH}} \times M_{\text{NaOH}} / W_0. \quad (3)$$

In order to test the methanol permeability, first a filler application was carried out to fill the pores of the nanofibrous membranes. For this purpose, Nafion[®]

117 solution (5%) was used as filler. The samples were immersed in Nafion solution for 5 min and then removed samples were dried in an oven at 80°C. This process was repeated for three times to ensure a smooth coating. Then the samples were subjected to a heat treatment at 125°C for 1 h. Before the methanol permeability test, each sample was immersed into distilled water for 24 h to obtain a fully swollen structure. Then the samples were mounted between the cells of a diffusion side-by-side cell (PermeGear). Each cell had a 50 mL volume and 15 mm orifice diameter. After the sample membrane was placed between the cell halves, a cell clamp is placed around them. One cell was filled with 2 M methanol solution, while the other was filled with distilled water. In addition, stirring magnets were put in each cell. The side-by-side cell assembly was placed onto magnetic stirrer and the liquids were stirred during the test to ensure homogeneity. The test was conducted at a constant temperature of 25°C inside a climate chamber. To determine the amount of methanol passing to the distilled water cell over time, 1.5 mL of water samples were extracted from the distilled water cell at specific intervals (30, 60, 90, and 180 min). Extracted water samples were analyzed in a GC-FID (Agilent Technologies 7820A) to determine the methanol concentration, based on chromatogram area values. Using the obtained methanol concentration data, the methanol permeability was calculated according to the following equation;

$$C_{B(t)} = AV_B^{-1}DKL^{-1}C_A(t - t_0), \quad (4)$$

where, DK (cm^2/s) is the methanol permeability coefficient, C_A (mol/l) and C_B (mol/l) is the methanol concentration in diffusion cells, A (m^2) the membrane surface area at the orifice, V_b (liter) the diffusion cell volume and L (cm) the membrane thickness.³⁴

To determine the statistical importance of the variations, analysis of variance (ANOVA) tests were applied. Additionally, Duncan method was chosen for Post Hoc evaluation. The results of the tests were a set of subsets of means, where in each subset means was found to be insignificantly different from one another. The results of the statistical analysis were given in the Supplementary Information file.

3 | RESULTS AND DISCUSSION

3.1 | Nanofiber production and morphology

The properties of the electrospinning solutions and the average nanofiber diameters of the resulting nanofibers

TABLE 1 Properties of polyvinyl alcohol (PVA) and PVA/Nafion solutions and resulting nanofiber diameters.

Sample	Viscosity (cP)	Conductivity ($\mu\text{S}/\text{cm}$)	pH	Average nanofiber diameter \pm SD (nm)
PVA	266.7	338	5.87	330.0 \pm 49.1
PVA + 5% SSA	333.3	6230	1.56	279.6 \pm 58.9
PVA + 10% SSA	266.7	12,240	1.28	277.9 \pm 68.7
PVA + 15% SSA	266.7	14,850	1.23	269.6 \pm 47.6
PVA/Nafion	93.3	1052	2.05	239.7 \pm 54.8
PVA/Nafion +5% SSA	133.3	2460	1.81	248.7 \pm 62.7
PVA/Nafion +10% SSA	133.3	3400	1.69	271.6 \pm 59.7
PVA/Nafion +15% SSA	133.3	4420	1.67	278.6 \pm 69.0

were given in Table 1. Additionally, SEM images and nanofiber diameter distribution histograms of nanofibers were illustrated in Figure 1. It was observed that PVA/Nafion solutions had lower viscosity compared to PVA solution, as expected, due to the lower viscosity of Nafion solution, which is the result of the inadequate chain entanglement of Nafion polymers. The incorporation of SSA, however, did not cause a significant change in the viscosity of the final solutions both for PVA and PVA/Nafion. The conductivity of PVA/Nafion solution was higher and the pH was lower compared to neat PVA solution because of the sulfonic acid groups of Nafion. The incorporation of SSA into the electrospinning solutions and the increase in SSA concentration led to an increase in the conductivity and decrease in the pH because of the increase in sulfonic acid group content.

When SEM images were examined, it was observed that smooth bead-free nanofibers could be obtained for PVA nanofibers at all SSA concentrations. It was shown that when SSA was incorporated into PVA solution, thinner nanofibers were obtained compared to neat PVA, most likely because of the increased conductivity. Statistically, when compared with One-Way ANOVA as shown in Table S1, there was a significant difference between the mean nanofiber diameters of PVA and SSA cross-linked PVA nanofibers ($p < 0.05$). On the other hand, according to the Duncan post-hoc test (Table S2), SSA cross-linked PVA nanofibers were found to be in the same subset and their nanofiber diameters were not

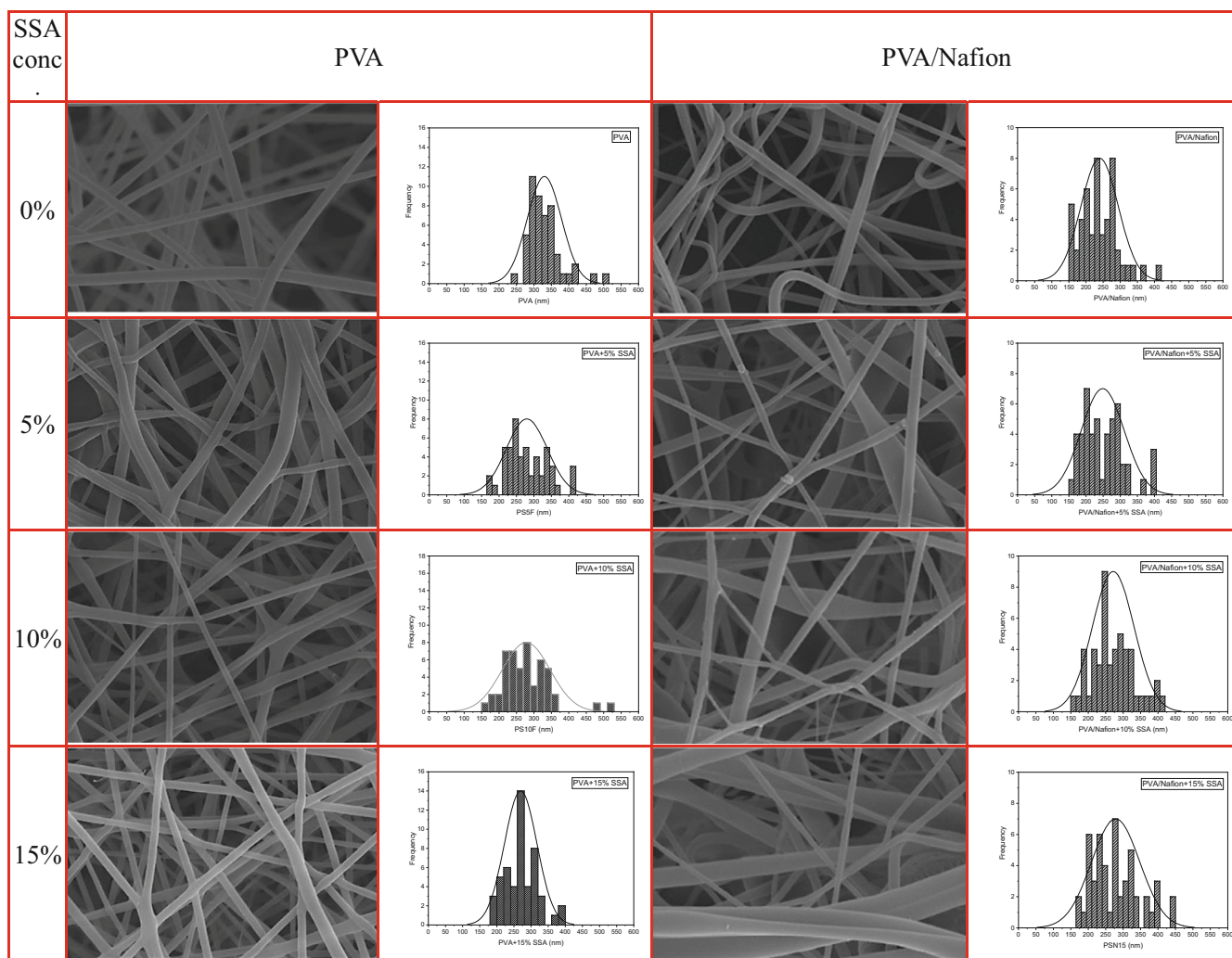


FIGURE 1 Scanning electron microscopic images and nanofiber diameter distribution histograms of neat and sulfo succinic acid (SSA) cross-linked polyvinyl alcohol (PVA) and PVA/Nafion nanofibers (50,000 \times magnification). [Color figure can be viewed at wileyonlinelibrary.com]

significantly different from each other. Therefore, SSA concentration had no effect on the average nanofiber diameter of PVA nanofibers.

Occasional bead formation was observed for SSA incorporated PVA/Nafion nanofibers, which was most likely due to the deterioration of the jet stability by the increased conductivity in addition to the low viscosity. Statistically, a One-Way ANOVA, as shown in Table S3, revealed a significant difference between the mean diameters of PVA/Nafion nanofibers ($p < 0.05$). According to Duncan post-hoc test (Table S4), PVA/Nafion and PVA/Nafion+5% SSA were in the same subset, and PVA/Nafion+15% SSA and PVA/Nafion+10% SSA were in another subset. On the other hand, nanofiber diameters of PVA/Nafion+10% SSA and PVA/Nafion+5% SSA were not significantly different from each other.

3.2 | FTIR analysis

In PVA nanofibers containing SSA, cross-linking was expected to occur through the esterification reaction between the carboxyl groups of SSA and the hydroxyl groups of PVA after the heat treatment. In this way, not only the stabilization of the PVA fraction was achieved, but also the sulfonation of PVA could be provided without the need for an additional post-sulfonating treatment. To prove this, FTIR analysis of the samples was carried out. FTIR transmittance spectra of PVA and PVA/Nafion nanofibers cross-linked with SSA were shown in Figures 2 and 3, respectively. In the spectrum of PVA, the 3100–3600 cm^{-1} band corresponded to the O–H stretching of intramolecular hydrogen bonds. It was observed that the intensity of this peak decreased in the samples cross-linked with SSA. This indicated that the hydroxyl groups

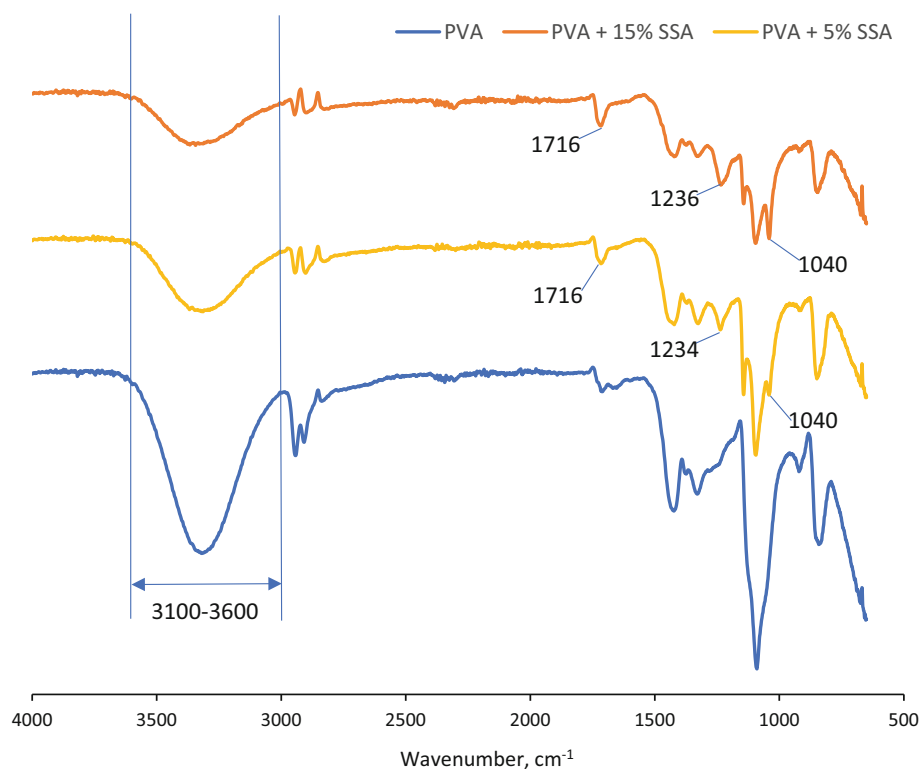


FIGURE 2 Fourier transfer infrared spectroscopy transmittance spectra of polyvinyl alcohol (PVA) and PVA + sulfosuccinic acid (SSA) nanofibers. [Color figure can be viewed at [wileyonlinelibrary.com](https://onlinelibrary.wiley.com/doi/10.1002/app.56346)]

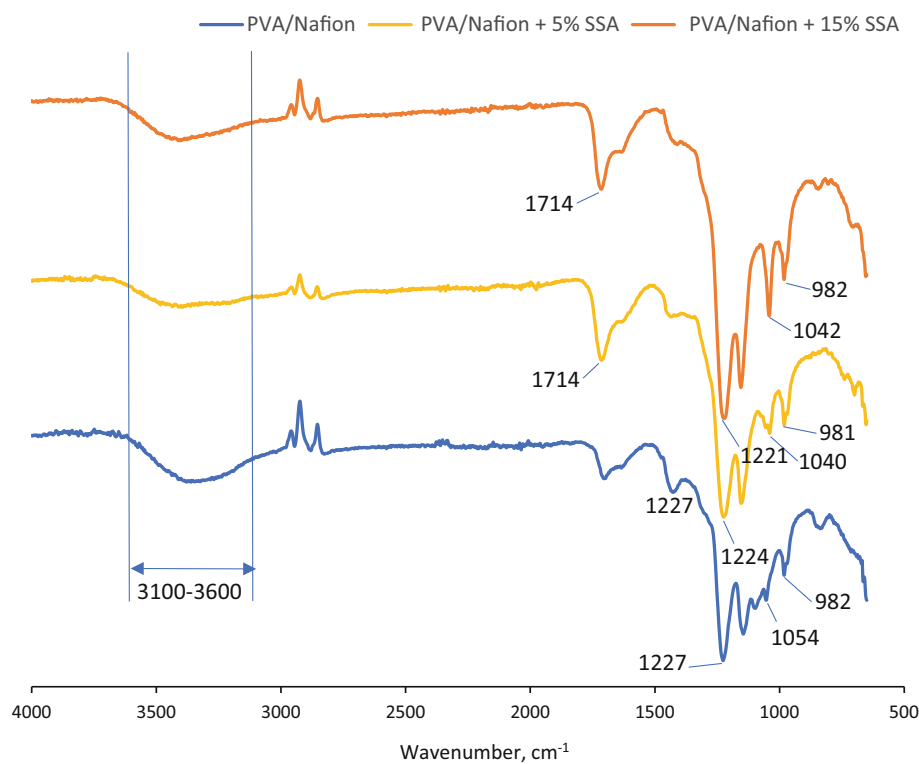


FIGURE 3 Fourier transfer infrared spectroscopy transmittance spectra of polyvinyl alcohol (PVA)/Nafion and PVA/Nafion+sulfosuccinic acid (SSA) nanofibers. [Color figure can be viewed at [wileyonlinelibrary.com](https://onlinelibrary.wiley.com/terms-and-conditions)]

of PVA decreased. The peaks appeared at 1716 cm^{-1} in PVA + SSA nanofibers were attributed to the C=O stretching in the ester group.⁴⁰ These results categorically proved that an esterification reaction occurred between the carboxyl groups of SSA and hydroxyl groups of PVA within nanofibers. In addition, in PVA + SSA nanofibers,

new peaks associated with asymmetric and symmetric S=O stretching of the $\text{—SO}^3\text{—}$ groups appeared at 1040 and 1234 cm^{-1} , respectively.^{41,42} The presence of this peak clearly showed the substitution of sulfonic acid groups into the nanofiber structure while cross-linking with SSA was carried out.

Similar to the FTIR spectrum of PVA nanofibers, the FTIR spectra of PVA/Nafion involves the 3100–3600 cm^{-1} band corresponds to the O–H stretching of intramolecular hydrogen bonds, but with a lower peak intensity. Also, the O–H peak for PVA nanofibers at 3310 cm^{-1} shifted to higher wavenumber (3380 cm^{-1}) for PVA/Nafion nanofibers, which was a result of the formation of additional hydrogen bonds between –OH groups of PVA and –SO₃H groups of Nafion.⁴³ This shift was observed to increase to higher wavenumbers (up to 3405 cm^{-1}) by the increase in SSA concentration, which might confirm the increasingly incorporation of –SO₃H groups into the nanofiber structure by SSA crosslinking. The same was also observed for pure PVA nanofibers after SSA crosslinking. SSA crosslinking of PVA fraction in PVA/Nafion nanofibers were observed by the peaks attributed to the ester bonds appeared at 1713 cm^{-1} . However, since Nafion peaks are dominant in the spectra (typical peaks at ~1200, 1143, and 980 cm^{-1} attributed to C–F bonds, at ~1050 cm^{-1} associated with the sulfonic acid groups)⁴⁴ the incorporation of additional sulfonic acid groups by SSA crosslinking could not be observed by the appearance of new peaks, due to overlapping.

3.3 | Thermogravimetric analysis

TGA analysis was carried out to assess the thermal resistance of PVA and PVA/Nafion nanofibers and their 15%

SSA cross-linked forms. TG and differential thermogravimetry (DTG) curves were illustrated in Figure 4. Thermogravimetric data derived from TG and DTG curves were given in Table 2. All the membranes showed three distinct degradation steps. The first stage was associated with the weight loss by the removal of unbound and bound water up to around 100°C. For neat PVA nanofibers, the second stage, started around 268°C, corresponded to the elimination of mainly H₂O by the loss of side groups of the polymer chain, and the third stage, started around 400°C, was attributed to the degradation of the polymer backbone.^{45–47} It was observed that the onset temperature and second stage peak degradation temperature of PVA + SSA nanofibers decreased, which was possibly because of the elimination of SSA based sulfonic acid groups in the second degradation stage. On the other hand, cross-linking with SSA increased the third stage peak degradation temperature, half decomposition temperature and resulting char fraction.^{41,48} A similar effect also applied to PVA/Nafion nanofibers. Due to Nafion-derived sulfonic acid groups, the onset temperature and therefore the second stage peak degradation temperature of PVA/Nafion nanofibers were lower than PVA nanofibers. SSA cross-linking of PVA/Nafion nanofibers further decreased the onset temperature corresponding to the increased sulfonic acid content, however, increased the half decomposition temperature and char fraction, which were also higher than PVA based samples because of the higher thermal stability of Nafion results

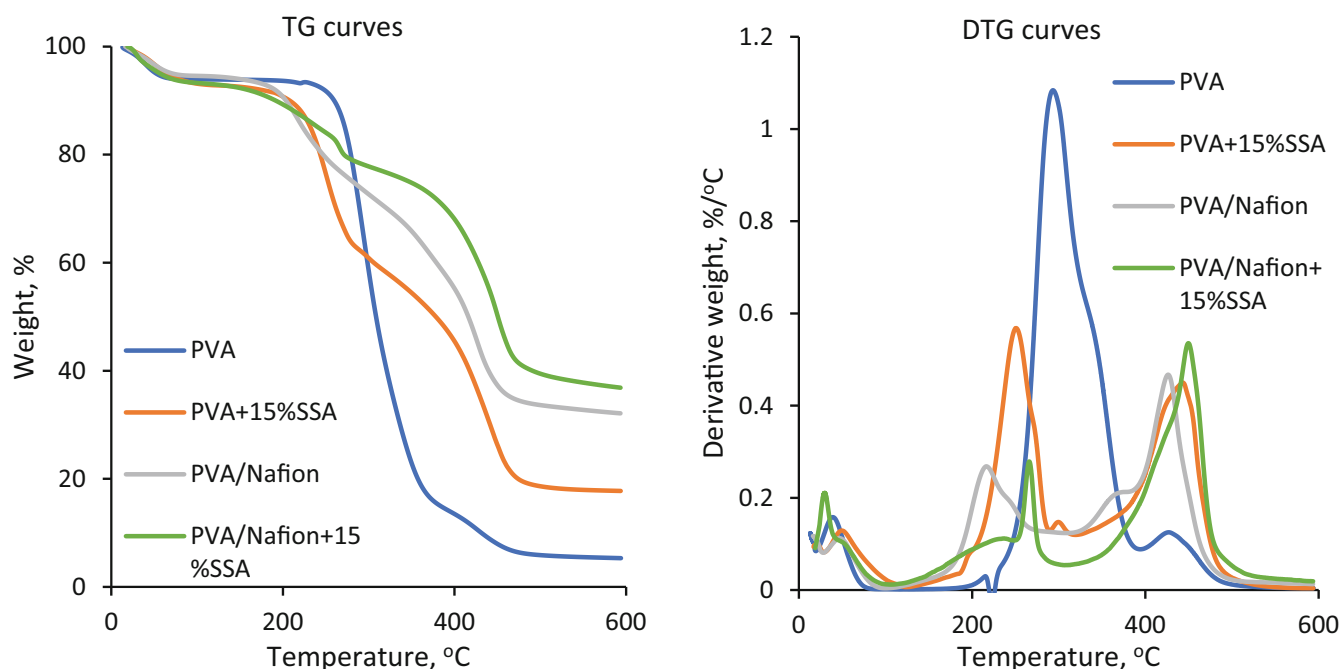


FIGURE 4 Thermogravimetry and differential thermogravimetry curves of neat and sulfosuccinic acid (SSA) cross-linked polyvinyl alcohol (PVA) and PVA/Nafion nanofibers. [Color figure can be viewed at [wileyonlinelibrary.com](https://onlinelibrary.wiley.com/doi/10.1002/polb.25636)]

TABLE 2 Thermogravimetric data of neat and sulfosuccinic acid (SSA) cross-linked polyvinyl alcohol (PVA) and PVA/Nafion nanofibers.

	Onset temperature, T_i (°C)	Peak degradation temperature of second step, T_{max2} (°C)	Peak degradation temperature of third step, T_{max3} (°C)	Half decomposition temperature, $T_{1/2}$ (°C)	Char fraction (%)
PVA	268	293	429	309	5.3
PVA + 15% SSA	224	250	443	378	17.8
PVA/Nafion	189	216	426	416	32.1
PVA/Nafion + 15% SSA	175	266	450	451	36.9

TABLE 3 Weight loss and swelling data of neat and sulfosuccinic acid (SSA) cross-linked polyvinyl alcohol (PVA) and PVA/Nafion nanofibers.

Sample	Weight lost in water (%)		Weight loss in methanol solution ^a (%)	Swelling in water ^b (%)
	At room temp.	At 100°C		
PVA	68.9	100.0	100	–
PVA + 5% SSA	6.7	18.3	14.9	355.7
PVA + 10% SSA	5.0	11.1	8.7	442.1
PVA + 15% SSA	4.8	11.1	9.3	454.5
PVA/Nafion	4.5	5.2	6.5	44.8
PVA/Nafion + 5% SSA	0.0	0.0	7.9	93.2
PVA/Nafion + 10% SSA	0.0	0.0	8.0	108.7
PVA/Nafion + 15% SSA	0.0	0.0	9.5	123.3

^aAt 80°C.^bAt room temperature.

from its perfluorocarbon backbone.⁴⁹ In conclusion, the thermal stability of PVA and PVA/Nafion nanofibrous membranes was shown to be improved by SSA cross-linking. Moreover, it should be mentioned that the thermal stability of both PVA + SSA and PVA/Nafion+SSA nanofibrous membranes met the requirements for the use in DMFCs, since the normal operating temperature of DMFCs is 80°C.⁵⁰

3.4 | Weight loss and swelling in water

The swelling and weight loss in water and methanol solution results were given in Table 3. Since PVA is soluble in water, a large weight loss was observed in water at room temperature and it was completely dissolved in boiling water and methanol solution, as expected. The stability of PVA nanofibers to water was improved significantly as a result of the SSA cross-linking. Whereas, although the samples cross-linked with 5% SSA concentration showed higher

weight loss, when the SSA concentration was further increased, the weight loss decreased, but the increasing SSA concentration did not significantly affect the weight loss.

The weight loss of neat PVA/Nafion nanofibers were found to be quite low, although PVA constitutes approximately 67% of the structure without any further stabilization. This was thought to be a clear indication of the formation of additional hydrogen bonds between –OH groups of PVA and –SO₃H groups of Nafion, as discussed in the results of FT-IR analysis. With the additional SSA cross-linking, the weight loss of PVA/Nafion nanofibers was completely eliminated.

In water at room temperature, the difference in the weight loss of PVA/Nafion, PVA + 15% SSA, PVA + 10% SSA and PVA + 5% SSA was not statistically significant at significance level of $\alpha = 0.05$, while their weight losses were significantly lower than PVA (Table S5). In boiling water, PVA/Nafion nanofibers showed significantly lower weight loss compared to PVA and SSA cross-linked PVA nanofibers (Table S6).

In the previous study,²⁹ PVA and PVA/Nafion nanofibers were stabilized by physical stabilization by heat treatment and chemical cross-linking by 1,2,3,4- butanetetracarboxylic acid (BTCA). Comparing the results of the present study where SSA was used for chemical cross-linking, similar weight loss was observed when PVA nanofibers were cross-linked with BTCA or SSA. On the other hand, PVA/Nafion nanofibers showed a certain weight loss when cross-linked with BTCA, but no weight loss was observed in the presence of SSA.

Swelling results showed that the increase in the SSA concentration led to a statistically significant increase in the swelling ratio for both PVA and PVA/Nafion nanofibers (Table S7) in general. On the other hand, it was also shown that no additional significant increase was achieved by the increase in the SSA concentration from 10% to 15% for PVA nanofibers. In fact, as the SSA concentration increased, the degree of swelling was expected to decrease because of the higher cross-linking density. For example, Kim et al.⁴³ investigated that the increase in the poly(styrene sulfonic acid-co-maleic acid) content led to a decrease in the water content of the cross-linked PVA film membrane. However, encountered exact opposite effect in the present study was quite likely stem from the higher solvation property of the sulfonic acid groups compared to PVA,⁴³ which increased the water retention and swelling ratio. A similar result was reported in the study of Sriruangrungrakamol and Chonkaew,⁴⁰ in which nanocellulose film membrane was cross-linked with SSA. They reported that at higher SSA concentrations (>3%), the increase in the amount of SSA increased the water uptake of the membrane. In another study, Rhim et al.³⁴ showed that the increase in the SSA content decreased the water content of cross-linked PVA film membranes prepared at 120 and 125°C until the SSA content reached 15%; and above this concentration the total water content of the membranes slightly increased because of the increase in the amount of sulfonic acid group. Further, Yoon et al.⁴¹ reported that the higher the SSA content the higher the water retention of the polyvinyl alcohol film membrane. In our case, it was revealed that the amount of ionic groups was much more effective on the swelling performance than the degree of cross-linking in the stabilization of PVA and PVA/Nafion nanofibers with SSA. It should also be added that the swelling degree of PVA/Nafion nanofibers were significantly lower than PVA nanofibers (Table S7), because of the hydrophobic polytetrafluoroethylene backbone of the Nafion polymer.

According to weight loss results, it could be envisaged that even lower SSA concentrations were suitable for the stabilization of PVA and PVA/Nafion nanofibers against water. However, since the preservation of the nanofibrous structure was required, the SEM images of the

samples after water treatments were investigated to analyze the resulting morphology changes, as shown in Figure 5. Since the nanofibrous membrane structure of neat PVA nanofibers was completely degraded in water, no SEM image was taken for neat PVA after water treatment. As a result of treatment with water (at room temperature or at 100°C), the PVA nanofibers gained a swollen, voluminous and partly fused structure, due to high swelling behavior. At 5% SSA concentration, it was observed that the dissolved PVA part filled the pores between the nanofibers by forming a film layer. This effect was also slightly observed for higher SSA concentrations. However, the nanofibrous structure was shown to be largely preserved for 10 and 15% SSA cross-linked PVA nanofibers and the degradation in the structure visually determined to be decreased as the SSA concentration increased. Therefore, although increasing the SSA concentration from 10% to 15% did not made a significant difference in terms of weight loss, it can be concluded that the use of 15% of SSA would be more adequate for preserving the nanofibrous structure of PVA nanofibers. For PVA/Nafion nanofibers, the nanofibrous structure were preserved even after the treatment with boiling water without a need of an additional cross-linking, which was due to the interaction between the hydroxyl and sulfonic acid groups within the structure, as aforementioned. Therefore, the treatment with SSA served the purpose of the incorporation of sulfonic acid groups to the PVA fraction rather than increasing the stability of the structure of PVA/Nafion nanofibers. It should be mentioned that partial bead formation was observed, especially at low SSA concentrations.

When the swelling results were compared with the previous study,²⁹ where crosslinking with BTCA and physical stabilization with heat treatment were investigated, it was seen that similar swelling results were obtained in PVA nanofibers when SSA or BTCA was used. On the other hand, lower swelling values were obtained in PVA/Nafion nanofibers as a result of cross-linking with SSA compared to BTCA. However, the swelling value remained higher than that of thermal stabilization.

Since the produced nanofibers were aimed to be used as polymer electrolyte membranes, especially in DMFCs, the nanofibrous structure was expected to be resistant to methanol solution. For this purpose, the samples immersed in 5 M methanol solution at 80°C for 24 h and the resulting weight loss and the change in the nanofiber morphology were shown in Table 3 and Figure 5, respectively. Again, neat PVA nanofibers were completely dissolved after soaking in methanol solution. It was observed that the samples cross-linked with SSA was largely preserved and the weight loss of the samples were

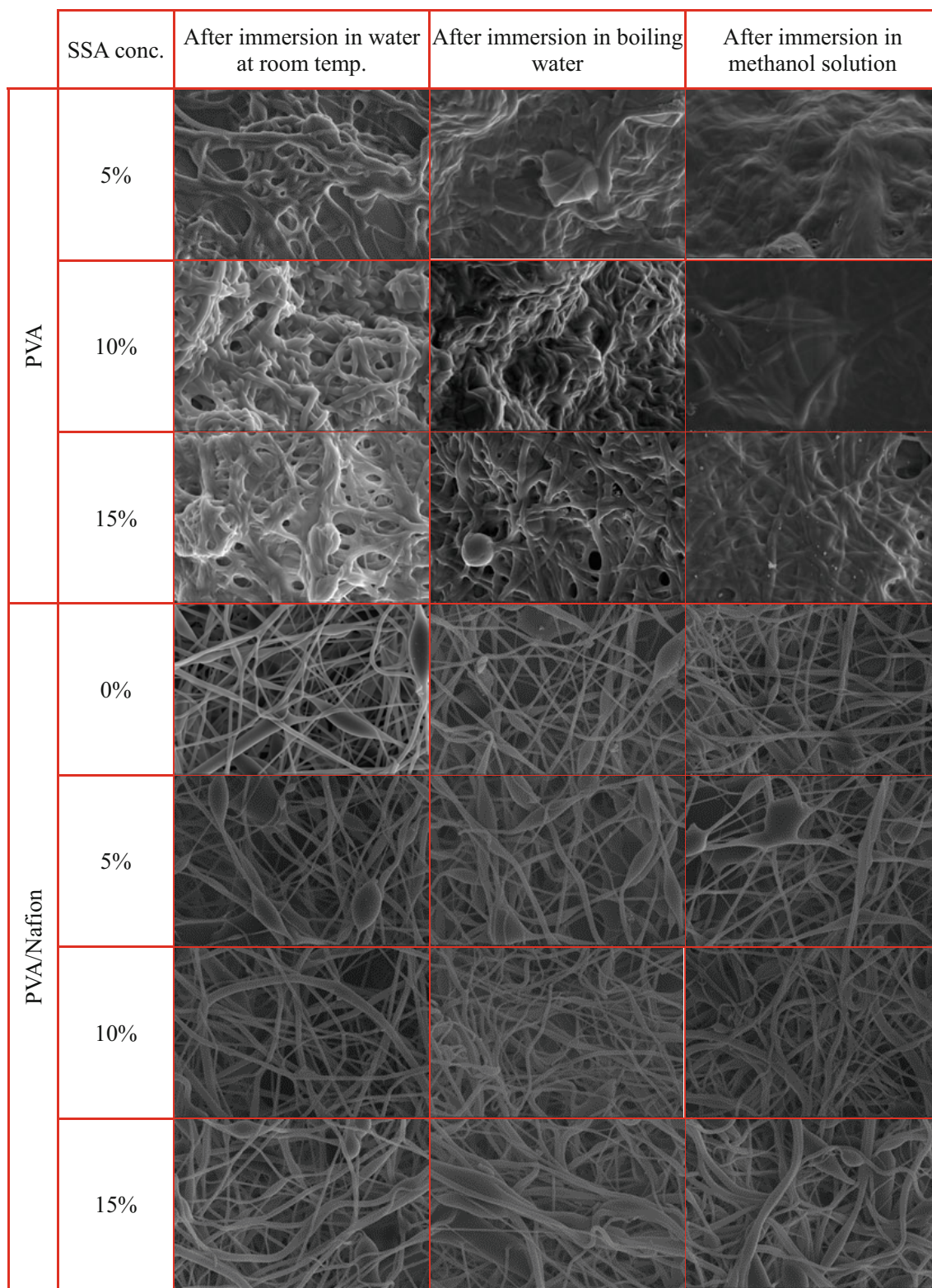


FIGURE 5 Scanning electron microscopic images of the samples after immersion into water and methanol solution (20,000 \times magnification). [Color figure can be viewed at wileyonlinelibrary.com]

shown to be similar regardless of nanofiber type and SSA concentration, except 5% cross-linked PVA nanofibers (Table S8) which showed higher weight lost due to

inadequate stabilization of the structure. Although SSA cross-linked PVA/Nafion nanofibers showed no weight loss under water environment, they possessed a certain

weight loss in methanol solution due to the dissolution of the hydrophobic backbone since methanol shows a higher affinity with the ether groups of the side chains.⁵¹ A higher deterioration in the nanofibrous structure were observed for 5% and 10% SSA cross-linked PVA nanofibers compared to water treatment. 15% SSA cross-linked PVA nanofibers, on the other hand, became swollen and fused but preserved their nanofibrous structure. The PVA/Nafion nanofibers, neat or cross-linked, visually shown to be quite stable to methanol solution treatment in terms of nanofibrous structure except for partial bead formation, as in water treatment tests.

3.5 | Ion exchange capacity and methanol permeability

IEC is an important parameter for the characterization of polymer electrolyte membranes which is related to the amount of ion exchangeable groups and it affects the ionic conductivity and water uptake of the membranes.⁵² The IEC of SSA cross-linked PVA and PVA/Nafion nanofibrous membranes was shown in Figure 6a. It was observed that the IEC of cross-linked PVA/Nafion nanofibers (1.46–3.98 mmol/g) was higher than those of PVA (0.51–1.61 mmol/g), for the same SSA concentration, and this difference was statistically significant (Table S9). This difference indicated a higher number of sulfonic acid groups due to the presence of Nafion

in the structure. The increase in the SSA concentration led to an increase in the IEC in general, through the incorporation of increasing amount of sulfonic acid groups. It was thought that, also the unreacted carboxylic acid groups of SSA might be the reason of the higher IEC values. The IEC results were in a good agreement with the swelling results. Again, for PVA nanofibers, no additional increase in the IEC was obtained by the increase in the SSA concentration from 10% to 15%, thus their difference was statistically insignificant (Table S9).

Methanol diffusion through polymer electrolyte membranes is undesirable because methanol crossover from the anode to the cathode negatively affects fuel cell performance. Therefore, the selection of membranes with lower methanol permeability is of importance in DMFC applications.⁵³ Since nanofibrous membranes have a highly porous structure, it will be beneficial to block the pores with filler materials to prevent additional fuel permeation through the pores. Therefore, in this study, the SSA cross-linked membranes were impregnated with Nafion solution, before the methanol permeability tests. However, for comparison, 15% SSA cross-linked PVA and PVA/Nafion nanofibrous membranes without a further Nafion impregnation was also tested. The results of the methanol permeability tests were shown in Figure 6b. It was shown that the unfilled membranes possessed higher methanol permeation due to the diffusion of methanol through the pores between the nanofibers. The filler application contributed to the reduction in methanol

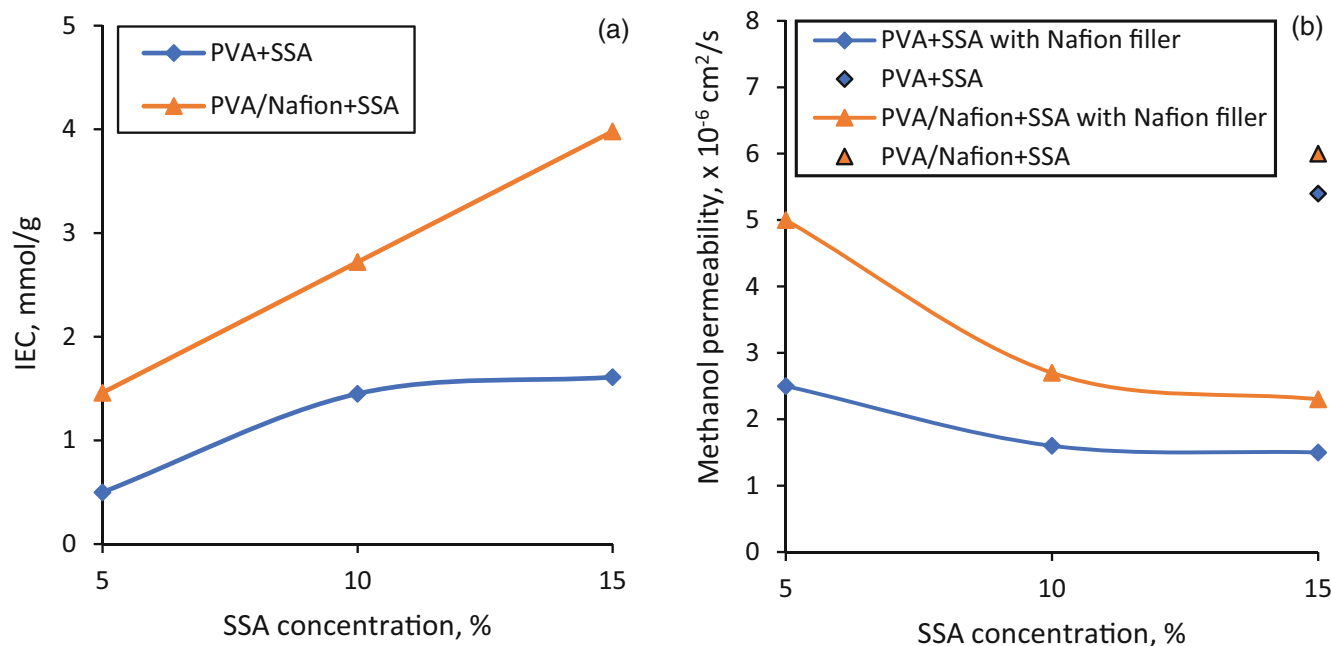


FIGURE 6 (a) Ion exchange capacity and (b) methanol permeability of sulfosuccinic acid (SSA) cross-linked polyvinyl alcohol (PVA) and PVA/Nafion nanofibers. [Color figure can be viewed at [wileyonlinelibrary.com](https://onlinelibrary.wiley.com)]

crossover. The methanol permeability was highly correlated with the increase of the SSA concentration. The higher the SSA concentration, the lower the methanol permeability. For a fully hydrated state, the methanol diffusion through the membrane is affected by the degree of swelling and microstructure of the membrane.⁵⁴ It was interesting that the methanol permeability of the membranes decreased although the water content of the cross-linked PVA and PVA/Nafion nanofibers increased with the increase in SSA content. In the study of Zhong et al.,⁵⁵ the same effect has been observed in which sulfonated polyether ether ketone (SPEEK) membranes were coated with cross-linked chitosan (CS) and the increase in the thickness of CS layer led to higher water uptake but lower methanol diffusion. This was explained by the smaller molecular size of water molecules compared to methanol, therefore the increase in CS content led to a preferential transport of small-sized water molecules. Moreover, in the study of Zhang et al.,⁵⁶ it was reported that the molecule with stronger polarity has higher flux for hydrophilic pores by citing Bhanushali et al.,⁵⁷ and showed that the flux for the transport diffusion of water was higher than methanol. Therefore, the lower polarity of methanol compared to water and increased hydrophilic character of SSA crosslinked nanofibers might lead to a decrease in methanol diffusion. It was also thought that the cross-linking network of the membranes due to SSA crosslinking was more effective in terms of the methanol permeability. The cross-linking of PVA led to a more rigid and dense structure, therefore the free volume which the methanol molecules could penetrate reduced and thus the methanol migration decreased.^{53,58} However this relationship was not linear. For both nanofiber types, the highest methanol permeability was obtained in the samples cross-linked with 5% SSA concentration. When the SSA concentration increased to 10%, the methanol permeability decreased significantly (36% reduction for PVA, 46% reduction for PVA/Nafion). The further increase in the SSA concentration led to an additional decrease in the methanol permeability but this decrease was much smaller. As a result, in the light of the aforementioned explanations, the decrease in methanol permeability by the increase in SSA content was possibly arisen from the synergistic effect of the higher selective tendency of the membranes to water than methanol and the cross-linked network that act as a methanol barrier.

The methanol permeability of SSA cross-linked PVA nanofibrous membranes were found to be lower compared to those of PVA/Nafion, although they showed higher water swelling. This could be due to the low methanol diffusion property of PVA polymer than Nafion²⁷ and higher flux of methanol than that of water through the hydrophobic pores.⁵⁶ The methanol permeability

results obtained in Nafion filled PVA + 15% SSA and PVA + 10% SSA membranes were found to be 1.5×10^{-6} and 1.6×10^{-6} cm²/s respectively, which were lower than the commercial Nafion 115 membrane tested to be 2.4×10^{-6} cm²/s⁵⁹ and was found to be comparable to that of commercial Nafion 117 membrane of 1.22×10^{-6} cm²/s.⁶⁰ Nafion filled PVA/Nafion+15% SSA was shown to exhibit similar methanol permeability to the commercial Nafion 155 membrane.

4 | CONCLUSIONS

PVA and PVA/Nafion based nanofibrous membranes were cross-linked with SSA and their characterization and performance properties such as stability in water and methanol solution, water swelling, IEC and methanol permeability were investigated.

Direct addition of SSA into the electrospinning solution did not significantly affect the nanofiber morphology; bead-free and smooth nanofibers were fabricated. Esterification of SSA with PVA and simultaneous inclusion of -SO₃H groups into the nanofibrous structure were proven by FTIR analyses. SSA cross-linking was also shown to increase the thermal stability of both PVA and PVA/Nafion nanofibrous membranes.

The water stability of the PVA nanofibrous membranes was improved by SSA crosslinking to a great extent. It was determined that PVA/Nafion nanofibers had high stability against water even without stabilization, and became completely stable against water after SSA cross-linking. PVA nanofibers had much higher water swelling compared to PVA/Nafion based ones. As the concentration of SSA increased, the degree of swelling increased. This showed that the number of ionic groups was more effective for the swelling of nanofibers compared to the cross-linking density. It was demonstrated that a high SSA concentration was necessary for PVA nanofibers in order to prevent the nanofibrous morphology from deteriorating after treatment with water. On the other hand the morphology of PVA/Nafion nanofibers were shown to be preserved even without cross-linking, due to the interaction between PVA and Nafion.

The IEC values of SSA crosslinked PVA/Nafion nanofibrous membranes were higher than cross-linked PVA nanofibers, and the IEC increased as the increase in SSA concentration, in general. Methanol permeability was investigated to be decreased by SSA crosslinking, attributed to the combined effect of the higher selective tendency of the membranes to water than methanol and the cross-linked network that act as a methanol barrier. Also, methanol crossover was shown to be lower for cross-linked PVA nanofibers compared to PVA/Nafion nanofibers.

It is worth noting that the mechanical properties and proton conductivity of the membranes and fuel cell tests under continuous operational conditions should be investigated in future studies.

AUTHOR CONTRIBUTIONS

Mert Işıl: Investigation (equal); writing – original draft (equal). **Ahmet Çay**: Funding acquisition (lead); project administration (lead); resources (lead); supervision (lead); validation (lead); writing – review and editing (equal). **Çiğdem Akduman**: Conceptualization (equal); formal analysis (equal); methodology (lead); writing – review and editing (equal). **Emriye Perrin Akçakoca Kumbasar**: Conceptualization (supporting); methodology (equal). **Hasan Ertaş**: Formal analysis (equal); methodology (supporting).

ACKNOWLEDGMENTS

The authors would like to gratefully acknowledge the financial support for this research received through Ege University, Scientific Research Projects Coordination Unit (Project no. FYL-2019-21411).

CONFLICT OF INTEREST STATEMENT

The authors declare that they have no known competing financial interests or personal relationships that could have appeared to influence the work reported in this paper.

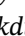
DATA AVAILABILITY STATEMENT

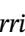
All data generated or analyzed during this study are included in this published article.

ORCID

Mert Işıl  <https://orcid.org/0000-0001-5330-4057>

Ahmet Çay  <https://orcid.org/0000-0002-5370-1463>

Çiğdem Akduman  <https://orcid.org/0000-0002-6379-6697>

Emriye Perrin Akçakoca Kumbasar  <https://orcid.org/0000-0001-5295-9131>

Hasan Ertaş  <https://orcid.org/0000-0002-5539-3732>

REFERENCES

- Y. Yan, X. Liu, J. Yan, C. Guan, J. Wang, *Energy Environ. Mater.* **2020**, *4*, 502.
- C. A. Bessel, K. Laubernds, N. M. Rodriguez, R. T. K. Baker, *J. Phys. Chem. B* **2001**, *105*, 1115.
- I. Shabani, M. M. Hasani-Sadrabadi, V. Haddadi-Asl, M. Soleimani, *J. Membr. Sci.* **2011**, *368*, 233.
- K. Halicka, J. Cabaj, *Int. J. Mol. Sci.* **2021**, *22*, 6357.
- F. Russo, R. Castro-Muñoz, S. Santoro, F. Galiano, A. Figoli, *J. Environ. Chem. Eng.* **2022**, *10*, 108452.
- C. Akduman, V. Demirel, F. Tezcan, *J. Appl. Polym. Sci.* **2021**, *138*, 50820.
- S. Wu, W. Shi, K. Li, J. Cai, C. Xu, L. Gao, J. Lu, F. Ding, *Int. J. Biol. Macromol.* **2023**, *239*, 124264.
- S. Wu, K. Li, W. Shi, J. Cai, *Carbohydr. Polym.* **2022**, *294*, 119756.
- R. Rasouli, A. Barhoum, M. Bechelany, A. Dufresne, *Macromol. Biosci.* **2019**, *19*, 1800256.
- V. Leung, F. Ko, *Polym. Adv. Technol.* **2011**, *22*, 350.
- F. Huang, Q. Wei, Y. Cai, in *Functional Nanofibers and Their Applications* (Ed: Q. Wei), Woodhead Publishing, Cambridge **2012**.
- N. Hamdan, A. Yamin, S. A. Hamid, W. K. W. A. Khodir, V. Guarino, *J. Funct. Biomater.* **2021**, *12*, 59.
- H. Chen, M. Huang, Y. Liu, L. Meng, M. Ma, *Sci. Total Environ.* **2020**, *739*, 139944.
- Y. N. Yusoff, N. Shaari, *Int. J. Energy Res.* **2021**, *45*, 18441.
- M. Tanaka, *Polym. J.* **2016**, *48*, 51.
- R. Xia, H. Zhou, Z. Zhang, R. Wu, W. P. Wu, *Polym. Eng. Sci.* **2018**, *58*, 2071.
- M. A. Kipnis, P. V. Samokhin, G. N. Bondarenko, E. A. Volnina, Y. V. Kostina, O. V. Yashina, V. G. Barabanov, V. V. Kornilov, *Russ. J. Phys. Chem. A* **2011**, *85*, 1322.
- L. Shen, Z. Sun, Y. Chu, J. Zou, M. A. Deshusses, *Int. J. Hydrogen Energy* **2015**, *40*, 13071.
- L. Wu, Z. Zhang, J. Ran, D. Zhou, C. Li, T. Xu, *Phys. Chem. Chem. Phys.* **2013**, *15*, 4870.
- Y. Yao, L. Ji, Z. Lin, Y. Li, M. Alcoutlabi, H. Hamouda, X. Zhang, *ACS Appl. Mater. Inter.* **2011**, *3*, 3732.
- H. Junoh, J. Jaafar, M. N. A. M. Norddin, A. F. Ismail, M. H. D. Othman, M. A. Rahman, N. Yusof, W. N. W. Salleh, H. Ilbeygi, *J. Nanomater.* **2015**, *2015*, 690965.
- B. Dong, L. Gwee, D. Salas-de la Cruz, K. I. Winey, Y. A. Elabd, *Nano Lett.* **2010**, *10*, 3785.
- C. Ding, Z. Qiao, *Ionics* **2022**, *28*, 1.
- N. W. DeLuca, Y. A. Elabd, *J. Membr. Sci.* **2006**, *282*, 217.
- H. L. Lin, S. H. Wang, C. K. Chiu, T. L. Yu, L. C. Chen, C. C. Huang, T. H. Cheng, J. M. Lin, *J. Membr. Sci.* **2010**, *365*, 114.
- H. L. Lin, S. H. Wang, *J. Membr. Sci.* **2014**, *452*, 253.
- S. Mollá, V. Compañ, *J. Membr. Sci.* **2011**, *372*, 191.
- S. Mollá, V. Compañ, E. Gimenez, A. Blazques, I. Urdanpilleta, *Int. J. Hydrogen Energy* **2011**, *36*, 9886.
- R. E. Zizhou, A. Çay, E. P. Akçakoca Kumbasar, C. Ö. Çolpan, *J. Ind. Text.* **2019**, *50*, 773.
- C. E. Tsai, C. W. Lin, B. J. Hwang, *J. Power Sources* **2010**, *195*, 2166.
- C. E. Tsai, C. W. Lin, J. Rick, B. J. Hwang, *J. Power Sources* **2011**, *196*, 5470.
- C. González-Guisasola, A. Ribes-Greus, *Polym. Test.* **2018**, *67*, 55.
- N. Kakati, J. Maiti, G. Das, S. H. Lee, Y. S. Yoon, *Int. J. Hydrogen Energy* **2015**, *40*, 7114.
- J. W. Rhim, H. B. Park, C. S. Lee, J. H. Jun, D. S. Kim, Y. M. Lee, *J. Membr. Sci.* **2004**, *238*, 143.
- O. Gil-Castell, D. Galindo-Alfaro, S. Sánchez-Ballester, R. Teruel-Juanes, J. D. Badia, A. Ribes-Greus, *Nanomaterials* **2019**, *9*, 397.
- I. Hayati, A. I. Bailey, T. F. Tadros, *J. Colloid Interface Sci.* **1987**, *117*, 205.
- W. K. Son, J. H. Youk, T. S. Lee, W. H. Park, *Mater. Lett.* **2005**, *59*, 1571.
- S. Mollá, V. Compañ, *J. Power Sources* **2011**, *196*, 2699.
- J. B. Ballengee, P. N. Pintauro, *J. Membr. Sci.* **2013**, *442*, 187.
- A. Sriruangrunghakamol, W. Chonkaew, *Polym. Bull.* **2021**, *78*, 3705.

- [41] J. Y. Yoon, H. Zhang, Y. K. Kim, D. Harbottle, J. W. Lee, *J. Environ. Chem. Eng.* **2019**, *7*, 102.
- [42] R. Zhang, B. Liang, T. Qu, B. Cao, P. Li, *Environ. Technol.* **2019**, *40*, 312.
- [43] D. S. Kim, M. D. Guiver, S. Y. Nam, T. I. Yun, M. Y. Seo, S. J. Kim, H. S. Hwang, J. W. Rhim, *J. Membr. Sci.* **2006**, *281*, 156.
- [44] Z. Liang, W. Chen, J. Liu, S. Wang, Z. Zhou, W. Li, G. Sun, Q. Xin, *J. Membr. Sci.* **2004**, *233*, 39.
- [45] B. Gupta, S. Anjum, S. Ikram, *Polym. Bull.* **2013**, *70*, 2709.
- [46] C. S. K. Figueiredo, T. L. M. Alves, C. P. Borges, *J. Appl. Polym. Sci.* **2009**, *111*, 3074.
- [47] F. C. Nascimento, L. C. V. Aguiar, L. A. T. Costa, M. T. Fernandes, R. J. Marassi, A. S. Gomes, J. A. Castro, *Polym. Bull.* **2021**, *78*, 917.
- [48] A. K. Sahu, G. Selvarani, S. D. Bhat, S. Pitchumani, P. Sridhar, A. K. Shukla, N. Narayanan, A. Banerjee, N. Chandrakumar, *J. Membr. Sci.* **2008**, *319*, 298.
- [49] S. Ryu, B. Lee, J. H. Kim, C. Pak, S. H. Moon, *Int. J. Energy Res.* **2021**, *45*, 19136.
- [50] D. Liu, Y. Xie, J. Zhong, F. Yang, J. Pang, Z. Jiang, *J. Membr. Sci.* **2022**, *650*, 120413.
- [51] C. S. Wu, F. Y. Lin, C. Y. Chen, P. P. Chu, *J. Power Sources* **2006**, *160*, 1204.
- [52] A. Z. Al Munsur, B. H. Goo, Y. Kim, O. J. Kwon, S. Y. Paek, S. Y. Lee, H. J. Kim, T. H. Kim, *ACS Appl. Mater. Interfaces* **2021**, *13*, 28188.
- [53] S. Zhong, X. Cui, Y. Gao, W. Liu, S. Dou, *Int. J. Hydrogen Energy* **2014**, *39*, 17857.
- [54] W. F. Chen, P. L. Kuo, *Macromolecules* **2007**, *40*, 1987.
- [55] S. Zhong, X. Cui, T. Fua, H. Na, *J. Power Sources* **2008**, *180*, 23.
- [56] Q. Zhang, J. Zheng, A. Shevade, L. Zhang, S. H. Gehrke, G. S. Heffelfinger, S. Jiang, *J. Chem. Phys.* **2002**, *117*, 808.
- [57] D. Bhanushali, S. Kloos, C. Kurth, D. Bhattacharyya, *J. Membr. Sci.* **2001**, *189*, 1.
- [58] M. Yoo, M. Kim, Y. Hwang, J. Kim, *Ionics* **2014**, *20*, 875.
- [59] M. Işılai, A. Çay, Ç. Akduman, E. P. Akçakoca Kumbasar, H. Ertaş, *Polym. Eng. Sci.* **2024**. <https://doi.org/10.1002/pen.26943>
- [60] S. Mondal, S. Soam, P. P. Kundu, *J. Membr. Sci.* **2015**, *474*, 140.

SUPPORTING INFORMATION

Additional supporting information can be found online in the Supporting Information section at the end of this article.

How to cite this article: M. Işılai, A. Çay, Ç. Akduman, E. P. A. Kumbasar, H. Ertaş, *J. Appl. Polym. Sci.* **2025**, *142*(2), e56346. <https://doi.org/10.1002/app.56346>